Communications of BAO, Vol. 73, Issue 2, 2026, pp. 359-362

Probing the Ionizing Sources in Extremely Metal Poor Galaxies: An X-ray to IR Study of IZw18

A.Amiri *[1,2] and B. D.Lehmer[2]

[1]School of Astronomy, Institute for Research in Fundamental Sciences (IPM), Tehran, P.O. Box 19395-5531, Iran
[2]Department of Physics, University of Arkansas, 226 Physics Building, 825 West Dickson Street, Fayetteville, AR 72701, USA

Abstract

The nearby blue compact dwarf IZw18 combines a gas-phase metallicity of only ∼3% solar with resolved sites of young star formation and a bright ultraluminous X-ray source (ULX). Its nebular He II λ4686 emission demands photons above 54.4 eV, which stellar populations alone struggle to supply. We ask whether the ULX closes the gap. We first fit the 0.12–100 μm photometry together with eleven optical line ratios using the LIGHTNING code and BPASS binary models, which gives the star-formation history and the intrinsic stellar spectrum. The fit is good for nearly all constraints but misses He II λ4686 by several standard deviations. We then fit archival *Chandra* and *XMM-Newton* spectra with three ULX descriptions (an advection-dominated disk, disk plus hot plasma, and a super-Eddington funnel plus Comptonisation), add each to the stellar spectrum, and re-run CLOUDY. The brighter *XMM-Newton*-epoch spectra, when combined with the hot-plasma or funnel prescriptions, lift the predicted He II λ4686/Hβ close to the observed value while leaving the other lines essentially unchanged. The ULX is therefore a plausible, but not exclusive, explanation; fast shocks and other hard sources cannot be excluded.

Keywords: *X-ray binaries – ultraluminous X-ray sources – stellar populations – galaxies: dwarf – galaxies: individual (IZw18)*

1. Introduction

Nebular He II λ4686 is produced by recombination of He^+, so it traces radiation at energies above 54.4 eV. Massive single stars, and even many binary population models, fall short of the observed He II λ4686 strength in metal-poor galaxies (e.g. Berg et al. 2018; Stanway & Eldridge 2019). Proposed remedies include stripped or rapidly rotating stars (Götberg et al. 2018), fast radiative shocks (Thuan & Izotov 2005; Izotov et al. 2012) and X-ray binaries, whose numbers per unit star formation rise at low metallicity (Basu-Zych et al. 2016; Lehmer et al. 2021). ULXs ($L_X \gtrsim 10^{39}\,\mathrm{erg\,s^{-1}}$) are the most luminous of these, but their extreme-ultraviolet output is not observed directly and depends sensitively on the assumed spectral shape (Kaaret et al. 2017; Simmonds et al. 2021).

IZw18 ($d = 18.2$ Mpc; Aloisi et al. 2007; $Z \approx 0.03\,Z_\odot$) is the ideal laboratory: one of the lowest-metallicity star-forming systems known, with a ULX in its north-west knot and a well-measured He II λ4686 line (Kehrig et al. 2015, 2016). Our aim is to build an ionising spectrum that is simultaneously consistent with the X-ray data, the UV-to-IR spectral energy distribution (SED), and the optical lines.

2. Data and Method

Stellar SED. We assembled 44 broadband images from GALEX, *Swift*, HST, SDSS, Pan-STARRS, 2MASS, JWST, *Spitzer*, WISE and *Herschel*, convolved them to a common 10″ resolution, and measured fluxes in a single elliptical aperture. Together with eleven emission-line ratios relative to Hβ (Kehrig et al. 2016; PMAS integral-field spectroscopy, re-reddened to observed fluxes) this gives 52 constraints. We fit them with LIGHTNING (Lehmer et al. 2024) using BPASS v2.2.1 binary models, an 8-bin piecewise-constant star-formation history (SFH), Draine & Li (2007) dust emission, Noll et al. (2009) attenuation, and CLOUDY

*amirnezamamiri@gmail.com, Corresponding author

nebular emission ($n_{\rm H} = 100\,{\rm cm^{-3}}$, a single metallicity of 0.03–0.10 $Z_\odot$ for stars and gas, free ionisation parameter).

X-ray spectra. We reduced the archival *Chandra* observation (ObsID 805, 2000) and the *XMM-Newton* EPIC-pn data (2002 and 2024), which bracket the ULX between a low state ($L_{\rm X} \approx 2 \times 10^{39}\,{\rm erg\,s^{-1}}$) and its typical elevated state ($\approx 1.2 \times 10^{40}\,{\rm erg\,s^{-1}}$). Three intrinsic ULX descriptions were fitted: (i) an advection-modified disk (DISKPBB), with $T(r) \propto r^{-p}$ and $p < 0.75$ expected for super-Eddington flows; (ii) DISKPBB+APEC, following Oskinova & Schaerer (2022), in which soft X-rays from hot superbubble gas supply He^+-ionising photons; (iii) a funnel-shaped super-Eddington photosphere (SIRF) plus COMPTT, following Garofali et al. (2024). For *Chandra*, DISKPBB gives $kT_{\rm in} \approx 0.9\,{\rm keV}$, $p \approx 0.72$ and an extrapolated He II-ionising rate of $Q_{\rm He\,II} \approx (0.6\text{–}1.6) \times 10^{48}\,{\rm photons\,s^{-1}}$; for *XMM-Newton* it prefers $kT_{\rm in} \approx 1.3\,{\rm keV}$ and $p \approx 0.62$ (Table 3 of the full draft).

Combined SED. Each ULX model, extrapolated into the extreme UV, was added to the best-fit stellar spectrum, and CLOUDY (C23) was re-run with the same density, metallicity and ionisation parameter. This treats stars and ULX as one source of photons, an approximation we tested by feeding the stellar-only SED through the same procedure: it reproduces the full LIGHTNING line ratios to near-equal quality, which is reasonable here because stellar populations younger than ∼100 Myr dominate the SED. We assume the ULX is associated with that young population.

3. Results

Stellar-only model. The SFH peaks at a look-back time of $\sim 10^7$ yr, consistent with the 10–30 Myr burst inferred from resolved JWST colour-magnitude diagrams (Bortolini et al. 2024). The model matches the photometry and every strong line ([O II], [Ne III], Hγ, [O III], Hα, [N II], [S II], [Ar III]) well, with modest tension in the auroral [O III] λ4363 line. The one real failure is He II λ4686: the model gives He II $\lambda4686/{\rm H}\beta = 0.002$ against 0.020 ± 0.004 observed, a deficit of $\sim 4.5\sigma$ in the line-ratio fit.

Adding the ULX. Table 1 and Fig. 1 summarise the outcome. The *Chandra*-epoch DISKPBB spectrum, being faint and soft, changes the line ratios negligibly (He II $\lambda4686/{\rm H}\beta = 0.002$). The *XMM-Newton*-epoch DISKPBB fit alone helps only slightly. In contrast, the two physically richer models give a large improvement: the disk plus hot plasma model (Oskinova & Schaerer 2022) predicts He II $\lambda4686/{\rm H}\beta = 0.024$ and the funnel plus Comptonisation model (Garofali et al. 2024) predicts 0.011, cutting the line-ratio χ^2 from about 40 to 18 and 24, respectively. The other lines move by only a few per cent, so the extra hard photons are not inconsistent with the ionisation state traced by [O III]/[O II] and [Ne III].

Ionising SED	He II $\lambda4686/{\rm H}\beta$	Residual (σ)	Line-ratio χ^2
Observed (Kehrig et al. 2016)	0.020 ± 0.004	–	–
LIGHTNING best fit	0.002	4.5	40.4
Stellar SED only (CLOUDY)	0.002	4.4	39.7
+ ULX, *Chandra* DISKPBB	0.002	4.4	39.4
+ ULX, *XMM* DISKPBB	0.002	4.3	37.7
+ ULX, *XMM* DISKPBB+APEC	0.024	−0.9	18.1
+ ULX, *XMM* SIRF+COMPTT	0.011	2.2	23.6

Table 1. Predicted He II $\lambda4686/{\rm H}\beta$ for each ionising spectrum, with the residual (data − model)/σ and the χ^2 over all eleven line ratios.

4. Discussion and Conclusions

Stellar populations alone, even with binaries, cannot produce the observed He II λ4686 in IZw18, but the same populations plus the measured ULX can, provided its spectrum is not a simple soft disk. The result depends on which X-ray epoch and which extrapolation into the unobserved EUV is adopted; the model choice, not the X-ray data quality, drives the difference. The *XMM-Newton* state is the more typical one for this source, so we regard the improved fits as representative, while the faint *Chandra* state shows that the contribution fluctuates with ULX activity.

Several caveats apply. The ULX is merged into a single combined SED rather than assigned to a specific age bin; the CLOUDY calculation assumes a single ionisation-bounded nebula; and the line data come from an aperture that differs from the photometric one. Independent evidence also points to other contributors:

doi: https://doi.org/10.52526/25792776-26.73.2-359

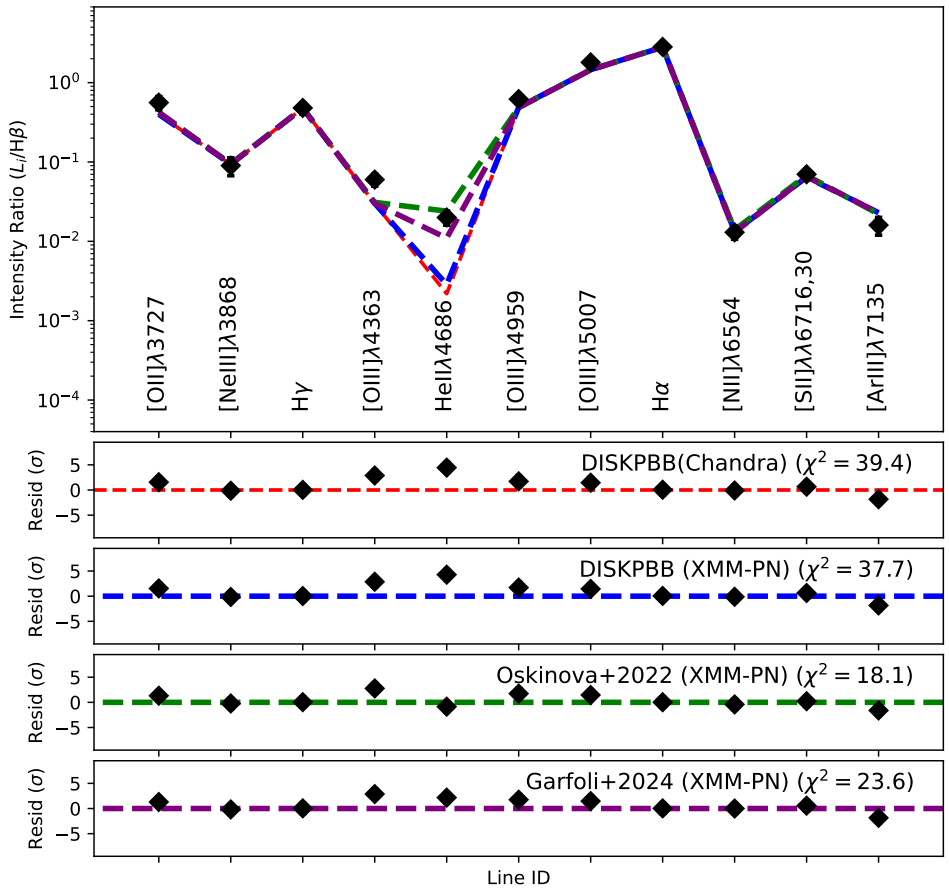

Figure 1. Observed (black diamonds) and predicted line ratios relative to Hβ for the stellar spectrum plus each ULX model. Red: *Chandra* DISKPBB; blue: *XMM-Newton* DISKPBB; green: *XMM-Newton* disk plus hot plasma; purple: *XMM-Newton* funnel plus Comptonisation. Lower panels give the residuals and the χ^2 of each model.

Wolf–Rayet stars in the north-west region, an ionised outflow, a redshift of about 30 km s^{-1} in He II λ4686 relative to Hα, and a spatial offset of the He II λ4686 gas from Hβ (Vaught et al. 2021; Arroyo-Polonio et al. 2024). Fast shocks therefore cannot be excluded as an additional source, although recent mid-infrared high-ionisation lines favour a hard radiation field from hot stars and X-ray sources over shocks alone.

We conclude that an accreting ULX, with realistic super-Eddington or hot-gas spectra, can naturally supply the missing He^+-ionising photons in IZw18 while preserving the fit to the other nebular lines. This strengthens the case that X-ray binaries and hot feedback-driven gas must be built into population-synthesis models used to interpret nebular spectra of metal-poor galaxies and their high-redshift analogues. Future work will include the X-ray source directly in the stellar population models and compare against shock models using the same data.

5. Acknowledgments

This work uses public data from *Chandra*, *XMM-Newton*, GALEX, *Swift*, HST, JWST, SDSS, Pan-STARRS, 2MASS, *Spitzer*, WISE and *Herschel*.

References

[1] Aloisi A., et al. 2007, ApJL, 667, L151

[2] Arroyo-Polonio A., et al. 2024, A&A, 687, A77

[3] Basu-Zych A. R., et al. 2016, ApJ, 818, 140

[4] Berg D. A., et al. 2018, ApJ, 859, 164

[5] Bortolini G., et al. 2024, A&A, 689, A146

[6] Draine B. T., Li A., 2007, ApJ, 657, 810

[7] Garofali K., et al. 2024, ApJ, 960, 13

[8] Götberg Y., et al. 2018, A&A, 615, A78

[9] Izotov Y. I., Thuan T. X., Privon G., 2012, MNRAS, 427, 1229

[10] Kaaret P., Feng H., Roberts T. P., 2017, ARA&A, 55, 303

[11] Kehrig C., et al. 2015, ApJL, 801, L28

[12] Kehrig C., et al. 2016, MNRAS, 459, 2992

[13] Lehmer B. D., et al. 2021, ApJ, 907, 17

[14] Lehmer B. D., et al. 2024, ApJ, 977, 189

[15] Noll S., et al. 2009, A&A, 507, 1793

[16] Oskinova L. M., Schaerer D., 2022, A&A, 661, A67

[17] Simmonds C., Schaerer D., Verhamme A., 2021, A&A, 656, A127

[18] Stanway E. R., Eldridge J. J., 2019, A&A, 621, A105

[19] Thuan T. X., Izotov Y. I., 2005, ApJS, 161, 240

[20] Vaught R. J. R., Sandstrom K. M., Hunt L. K., 2021, ApJL, 911, L17